Biotechnology and Bioprocess Engineering
https://doi.org/10.1007/s12257-026-00264-8

RESEARCH PAPER

Non-invasive online monitoring of polyol lipid production with *Aureobasidium pullulans* using fluorescence measurement

Max Daniel Dicke[1,4] · Noémie L. J. Carls[1] · Philipp Kohl[2,4] · Marie Dielentheis-Frenken[2,3] · Lars M. Blank[2,4] · Valentin Steier[1,4] · Marcel Mann[1,4] · Till Tiso[3,4] · Jørgen Barsett Magnus[1,4]

Received: 19 August 2025 / Revised: 20 January 2026 / Accepted: 25 January 2026
© The Author(s) 2026

Abstract
Polyol lipids (PLs) are biosurfactants produced by *Aureobasidium pullulans*, offering a promising, sustainable alternative to conventional surfactants from crude oil or palm oil. Online monitoring of product formation allows rapid process intensification. In this study, a new online monitoring method for PL formation is presented. Extracellular PL production was characterized in shake flasks using online monitoring of the respiratory activity. Three distinct phases of the process were identified: growth, PL production on glucose, and PL production on pullulan. With PL being fluorescent, an online fluorescence monitoring was developed. Therefore, 2D fluorescence spectra were recorded of PL solutions, revealing characteristic fluorescence. Based on these findings, specific wavelength combinations were evaluated for their online monitoring suitability during microtiter plate cultivations. Fluorescence measured at 540/580 nm ($\lambda_{ex}/\lambda_{em}$) correlates well with the amount of PLs produced. Online fluorescence monitoring of PL-producing and non-producing strains revealed strong differences in fluorescence signals, validating the chosen wavelength combination. The here presented online product analytics minimizes analysis time, supports miniaturized and parallelized strain comparisons, and not at least may contribute to future process intensification.

Keywords Fluorescence · Polyol lipids · Liamocin · Biosurfactant · *Aureobasidium pullulans* · Respiratory activity

1 Introduction

Surfactants are surface-active molecules that are used in a wide range of personal care and cleaning products, such as detergents or hand dishwashing liquids, due to their surface activity [1]. As most of the surfactants currently used are synthetic surfactants derived from petrochemicals or palm oil [2], their production contributes to global pollution and climate change.

Biosurfactants are surfactants excreted by microorganisms during biological synthesis, offering an environmentally friendly alternative to conventional surfactants due to their biodegradability and often low toxicity. They are mainly classified by their chemical structure and their microbial origin [2]. Their amphiphilic structure consists of a hydrophobic moiety based on saturated or unsaturated hydrocarbon chains or fatty acids and a hydrophilic moiety, like carboxylic acids, mono-, di-, or polysaccharides, or ionic structures like peptide cations or anions [2].

Glycolipids are the best-studied microbial surfactants [2, 3] and comprise the greatest share of commercially available microbial biosurfactants [4] with sophorolipids and rhamnolipids being the best-known representatives. Sophorolipids consist of a sophorose glycone and a C_{16} or C_{18} fatty acid tail and are mainly produced by *Starmerella bombicola* [4, 5]. Rhamnolipids are comprised of one or two rhamnose units linked to one or two 3-hydroxy fatty acid moieties, which can be produced in industrially relevant

✉ Jørgen Barsett Magnus
jorgen.magnus@avt.rwth-aachen.de

1 Aachener Verfahrenstechnik – Chair of Biochemical Engineering, RWTH Aachen University, 52074 Aachen, Germany

2 Institute of Applied Microbiology (iAMB), RWTH Aachen University, 52074 Aachen, Germany

3 Systems Biotechnology, Technical Faculty, Bielefeld University, 33615 Bielefeld, Germany

4 Bioeconomy Science Center (BioSC), 52425 Jülich, Germany

Published online: 09 February 2026

titers using *Pseudomonas* sp. [6]. Since January 2024, the first full industrial production plant for rhamnolipids has been in operation [7]. Polyol lipid (PL) biosurfactants (also known as liamocins) are another novel type of glycolipid biosurfactant produced by *Aureobasidium pullulans* [8].

A. pullulans is a yeast-like fungus from the *Ascomycota* division [9]. *Aureobasidium* spp. occur ubiquitously and exhibit polyextremotolerance, such as tolerance against extreme pH values or high salt concentrations [10, 11]. Its physiological attributes make *Aureobasidium* a promising genus for the application as an industrial microbe in an economically competitive biobased industry [12]. Due to its ability to secrete a wide range of enzymes, *Aureobasidium* can metabolize various complex carbon sources, such as hemicellulose, lignin breakdown products, and agricultural biomass, in addition to commonly used sugars [10, 13, 14]. *Aureobasidium* spp. can produce a variety of products, including PLs, pullulan, polymalic acid, melanin, or siderophores [8, 15–18]. Due to its melanin-producing capabilities, *A. pullulans* is considered a black yeast [19]. *A. pullulans* has been utilized for the production of the exopolysaccharide pullulan on an industrial scale since the 1970 s [15].

PL biosurfactants are another prominent secondary metabolite produced by *Aureobasidium* spp. [20]. Production and secretion of PLs by various *Aureobasidium* strains were first described by Kurosawa et al. in 1994 [8]. The complete structure of PLs was published in 2013 by Price et al. [21]. PLs consist of a single hydrophilic polyol head group, which is linked to an oligo-dihydroxydecanoic acid (DDA) by an ester bond [14, 21, 22]. DDAs are polyesters composed of three or four 3,5-dihydroxydecanoic acids, with the first fatty acid potentially being O-acetylated [20, 21]. They are synthesized as a precursor to PLs and thus are a part of the resulting congener mix produced [20]. The head group of PLs can vary between mainly mannitol or arabitol and other polyols like threitol or glycerol. The congener distribution of the produced PLs can be influenced by the supplementation of polyols to the cultivation medium [22].

As an alternative to complex media used previously for PL production, Haala et al. [23] developed and optimized a defined minimal medium for PL production to allow for a targeted investigation of alternative carbon sources and the metabolic pathway to identify targets for genetic optimization. After the statistical optimization of PL titer and yield using a Design-of-Experiment approach, 41 g L^{-1} PLs were produced by *A. pullulans* strain NRRL 62042 with the optimized version of the medium [23].

The amphiphilic structure of PLs results in great potential for application as biosurfactants. For PLs, a reduction of surface tension of water from 73 mN m^{-1} to around 30 mN m^{-1} was reported [24, 25], which is comparable to the performance of rhamnolipids [26]. In addition, PLs also exhibit antibacterial activity against *Streptococcus* spp. [27] and possess anticancer properties [24, 28]. Due to their high density, PLs have been termed "heavy oils" in the past [24], and their secretion results in the formation of an additional oil-like phase in the culture broth, which is beneficial for downstream processing. Interestingly, the oil-like PL phase produced by various strains of *A. pullulans* was described as highly fluorescent [24], which could potentially be used to monitor its formation with non-invasive fluorescence measurements.

Online measurements during microbial cultivations offer several advantages: They can be run in a non-invasive manner, resulting in a significant reduction of sampling efforts, no disturbances associated with manual sampling, and higher process autonomy. Combining online monitoring methods with small-scale cultivation systems, such as microtiter plates (MTPs) and shake flasks, generates higher experimental throughput for process optimization compared to lab-scale bioreactors. This is especially useful in strain screening during early process development.

Fluorescence measurement offers non-invasive online monitoring of key process parameters in bioprocess development and has been successfully applied for monitoring the formation and autofluorescent properties of molecules, such as vitamins, proteins, and cofactors [29, 30]. The BioLector technology enables high-throughput online monitoring of fluorescence and scattered light in shaken MTP cultures [31]. This non-invasive measurement technique is widely used in bioprocess development [32, 33]. Typical applications include the online monitoring of protein formation with fluorescent protein tags such as green fluorescent protein, yellow fluorescent protein, or mCherry [32, 34]. The formation of microbial products like undecylprodigiosin and actinorhodin pigments was also monitored previously using an autofluorescence signal in *Streptomyces coelicolor* [35]. With online 2D fluorescence spectroscopy, more diverse spectral dynamics during cultivation can be revealed compared to the widely applied monitoring of single wavelength combinations [36]. Berg et al. [37] used this technique for the prediction of culture parameters in cultivations of *Ogataea polymorpha* (formerly known as *Hansenula polymorpha*) using multivariate data analysis without sampling.

Another widely used online monitoring parameter in bioprocesses is the respiratory activity [38–40]. With the oxygen transfer rate (OTR), biological phenomena like a second substrate limitation (e.g., nitrogen) or the depletion of the main carbon source can be identified during cultivation [38]. The respiratory quotient (RQ) of carbon dioxide transfer rate (CTR) and OTR provides information on the

degree of reduction of the utilized carbon source and the produced metabolites [41]. Combining the online monitoring of gas transfer rates and fluorescence provides further valuable insights into bioprocesses such as the differentiation of different metabolic phases with these signals [35, 40–42].

This study evaluates the possibility of employing online fluorescence measurement for monitoring PL formation in small-scale cultivations of *A. pullulans* NRRL 62042. For this, wavelength combinations identified by recording 2D fluorescence spectra of the PL phase were used for monitoring during cultivation.

2 Materials and methods

2.1 Microorganisms

For PL production, the wild-type strain *A. pullulans* NRRL 62042 was cultivated. A second, genetically modified strain, *A. pullulans* VA.Y1, was constructed by Dielentheis-Frenken et al. (unpublished data) by deleting the $PKSI_{PL}$ gene encoding a polyketide synthase (GenBank accession number: KAK6005261.1) in the PL production pathway of the wild-type strain NRRL 62042 (as illustrated in Fig. S1). Deleting $PKSI_{PL}$ abolishes PL synthesis.

2.2 Media and cultivation

Cryo-cultures of *A. pullulans* were prepared in yeast extract peptone (YEP) medium containing 20 g L^{-1} glucose, 20 g L^{-1} peptone, and 10 g L^{-1} yeast extract and stored with 50% glycerol at −80 °C. Precultures were inoculated with 10 µL cryopreserved culture per mL and were cultivated in YEP medium for 22 h in 250 mL shake flasks with a filling volume of 20 mL at 30 °C, with a shaking diameter of 50 mm and a shaking frequency of 350 rpm.

To avoid process variation due to complex components like yeast extract [43], a defined minimal medium for PL production (MLP medium, adapted from Haala et al. [23]) was used in this work. The MLP medium contained 1 g L^{-1} NaCl, 1 g L^{-1} K_2HPO_4, 0.8 g L^{-1} $MgSO_4 \times 7\ H_2O$, 0.95 g L^{-1} NH_4NO_3, and 120 g L^{-1} glucose as well as 1 mL vitamin solution and 10 mL trace element solution per liter of medium. To prevent struvite precipitation, $MgSO_4$ was added to the medium right before inoculation [44]. The pH value of the completed medium was adjusted to 6.5 with 5 M NaOH. The vitamin solution contained 0.05 g L^{-1} of D-biotin, 1 g L^{-1} of D-calcium pantothenate, 1 g L^{-1} of nicotinic acid, 25 g L^{-1} of myo-inositol, 1 g L^{-1} of thiamine hydrochloride, 1 g L^{-1} of pyridoxol hydrochloride, and 0.2 g L^{-1} of para-aminobenzoic acid. The trace element solution consisted of 1.5 g L^{-1} of ethylenediaminetetraacetic acid, 0.45 g L^{-1} of $ZnSO_4 \times 7\ H_2O$, 0.10 g L^{-1} of $MnCl_2 \times 4\ H_2O$, 0.03 g L^{-1} of $CoCl_2 \times 6\ H_2O$, 0.03 g L^{-1} of $CuSO_4 \times 5\ H_2O$, 0.04 g L^{-1} of $Na_2MoO_4 \times 2\ H_2O$, 0.45 g L^{-1} of $CaCl_2 \times 2\ H_2O$, 0.3 g L^{-1} of $FeSO_4 \times 7\ H_2O$, 0.10 g L^{-1} of H_3BO_3, and 0.01 g L^{-1} of KI. Chemicals were purchased from Carl Roth GmbH & Co. KG. The colorless nature of this medium is also beneficial for online monitoring in this work, as no strong interference with fluorescence measurements is expected.

Main cultures were carried out using MLP medium [23]. Prior to inoculation, precultures were centrifuged (2,680 × g, 15 min, 4 °C), and the resulting cell pellets were resuspended in MLP medium to a starting optical density of 0.2.

2.3 MTP cultivations

MTP main cultures were cultivated in an in-house-built cultivation device (µRAMOS-Biolector combination) capable of monitoring oxygen transfer, scattered light, and fluorescence [42] using 48-well MTPs with a transparent bottom (M2P-MTP-R48-B, Beckman Coulter GmbH). Additional MTPs for offline sampling (M2P-MTP-R48-OFF, Beckman Coulter GmbH) were cultivated in a temperature-controlled incubation hood (Kuhner AG). All MTPs were sealed with a self-adhesive film (HJ-BIOANALYTIK GmbH) that allows for aeration. Each online monitored main culture was conducted in six biological replicates inoculated with the same pre-culture. All MTPs were cultivated at a shaking frequency of 1,000 rpm with a shaking diameter of 3 mm and a filling volume of 1 mL per well at 30 °C. Fluorescence was measured at 540 nm (λ_{ex}) and 580 nm (λ_{em}) with an integration time of 600 ms and a slid bandwidth of 8 nm. For more clarity, the fluorescence was blanked by setting intensities to zero after 24 h. This was done because the fluorescence signal was influenced by the growth of the organism, and the majority of PL formation is known to happen after cell growth [23, 24].

2.4 Shake flask cultivation

Shake flask cultivations were performed with eight parallel biological replicates, using the Transfer-Rate Online Measurement (TOM, Kuhner Shaker GmbH) [40], with a filling volume of 20 mL in 250 mL shake flasks, a shaking frequency of 350 rpm, at a shaking diameter of 50 mm, at 30 °C for 12 days.

2.5 Offline analytics

2.5.1 Sampling procedure

For sampling during shake flask cultivation, one flask was taken out of the incubator at a time. The whole culture was then transferred to a 50 mL centrifugation tube, and 3 mL of the culture was used for cell dry weight (CDW) determination in technical triplicates. To collect leftover PLs from the shake flask wall, each flask was thoroughly rinsed with 10 mL of acetonitrile (≥99.5% purity). After centrifugation of the remaining culture volume (2,680 × g, 20 min, room temperature) the supernatant was discarded. For PL recovery, the acetonitrile used for rinsing was mixed with the PL phase and the cell pellet. The resulting liquid phase was used for PL quantification.

For each sampling time point during MTP cultivations, three wells were sampled. For each sampled well, the entire well volume was transferred into a reaction tube and centrifuged (10 min, 21,100 × g, 4 °C). The supernatant was then used for pullulan and glucose determinations. Each well was thoroughly rinsed with 1 mL of acetonitrile (≥99.5% purity) to remove any remaining PL. The acetonitrile used for rinsing was then mixed with the remaining PL phase and the cell pellet, and the resulting liquid phase was used for PL determination.

2.5.2 Measurement of the optical density

The optical density (OD_{600}) was determined at a wavelength of 600 nm *via* a Genesys 20 photometer (Thermo Scientific GmbH). The culture broth was diluted with a 9 g L^{-1} NaCl solution to values between 0.1 and 0.3 before the measurement.

2.5.3 CDW

To determine the CDW of cultivation samples, 1 mL of culture broth was transferred to a pre-weighed reaction tube and subsequently centrifuged (10 min, 21,100 × g, 4 °C). For PL removal, the remaining cell pellet was washed with 50% ethanol (v_{EtOH}/v_{H2O}) after centrifugation. After washing, another centrifugation step was performed (10 min, 21,100 × g, 4 °C). The supernatant was discarded, and the remaining cell pellet was dried for at least 24 h at 80 °C until constant weight. To account for cell damage caused by ethanol, a correction factor of 1.52 was applied, which was determined by Haala et al. [23]. CDW of all samples was determined with three technical replicates.

2.5.4 Measurement of the pH value

The pH value was determined with a pH Meter (Hanna Instruments) using a pH probe (Mettler-Toledo) at room temperature. All pH measurements were performed as single measurements.

2.5.5 Determination of PL content

PL amounts were determined gravimetrically. For this, a pre-weighed reaction tube was filled with 1 mL of the PL containing acetonitrile, which was used for rinsing of the culture vessel and the PL extraction. The solvent was evaporated under a fume hood at room temperature until the weight of the tube was constant. The PL content of all samples was determined in triplicates (technical triplicates for shake flask cultivations, biological replicates for MTP cultivations).

2.5.6 Pullulan determination

For pullulan precipitation, the supernatant of each sample was mixed with ethanol (96 vol%) in a ratio of 1:1 (v/v) in a pre-weighed reaction tube. The tubes were centrifuged, and the supernatant was discarded. The remaining pullulan pellet was dried for at least 24 h at 80 °C until weight consistency. The pullulan content of all samples was determined in technical triplicates.

2.5.7 Glucose determination

Glucose concentrations were determined by high-performance liquid chromatography (HPLC) in single measurements. Culture broth supernatants were filtered (0.2 µm PET membrane) and subsequently analyzed in a Thermo Fisher Ultimate 3000 HPLC System (Thermo Fisher Scientific) using a Rezex ROA-Organic Acid H+ (8%) LC Column 300 × 7.8 mm (Phenomenex Inc.) and a RefractoMax 520 RI detector (Thermo Fisher Scientific). The mobile phase consisted of 25 mM H_2SO_4 with a flow rate of 0.8 mL min^{-1} at 85 °C. Samples were diluted with deionized water if necessary.

2.6 2D-fluorescence spectroscopy and data processing

2D-fluorescence spectra were recorded using an in-house-built device developed by Berg et al. [36]. Before measurement, samples were transferred into a 48-well round well MTP with a transparent bottom (M2P-MTP-R48-B, Beckman Coulter GmbH) and sealed with an air-tight self-adhesive film (SealPlate STR-SEAL-PLT, Excel Scientific

Inc.) to prevent solvent evaporation during measurement. Spectroscopic measurements were performed at a shaking frequency of 1,000 rpm with the following settings: excitation wavelength range = 270–700 nm, excitation step size = 10 nm, emission wavelength range = 270–700 nm, emission step size = 5 nm, integration time = 600 ms. Difference spectra were generated by subtracting spectra of solvent samples containing no PLs from spectra of PL-containing samples. Measured intensities in areas of scattered light ($\lambda_{ex} = \lambda_{em}$) were disregarded for visualization purposes.

3 Results and discussion

3.1 Characterization of PL production

In the first step, PL production was characterized in shake flasks. Cultures were monitored using the Kuhner TOM, which enables monitoring of OTR and CTR as well as the RQ [40]. Time-resolved data recorded during this cultivation are shown in Fig. 1.

PL production can be divided into three distinct phases: growth (phase I), simultaneous PL and pullulan production on glucose (phase II), and PL production on residual pullulan (phase III). In the first 12 h of phase I, respiration activity (OTR and CTR, Fig. 1A) increased exponentially, indicating growth of *A. pullulans*. After 12 h, the OTR increased at a slower rate, while the CTR continued to increase exponentially, resulting in a sudden change in the RQ from 1.3 to a value of 1.9. The RQ provides information on the degree of reduction of the utilized carbon source and the produced metabolites [41]. In general, RQ values above 1.0 (CTR > OTR) indicate the production of products that are more reduced than the substrate. This shift in RQ can be explained by the diauxic growth on two different nitrogen sources, with ammonium nitrate as the nitrogen source. Ammonium is consumed first, followed by the consumption of the highly oxidized nitrate [23]. This brings additional oxygen into the system compared to ammonium; the oxygen consumption is lowered, resulting in a shift towards higher RQ values. Both OTR and CTR peaked after 18 h of cultivation with values of 16 and 24 mmol L^{-1} h^{-1}, subsequently

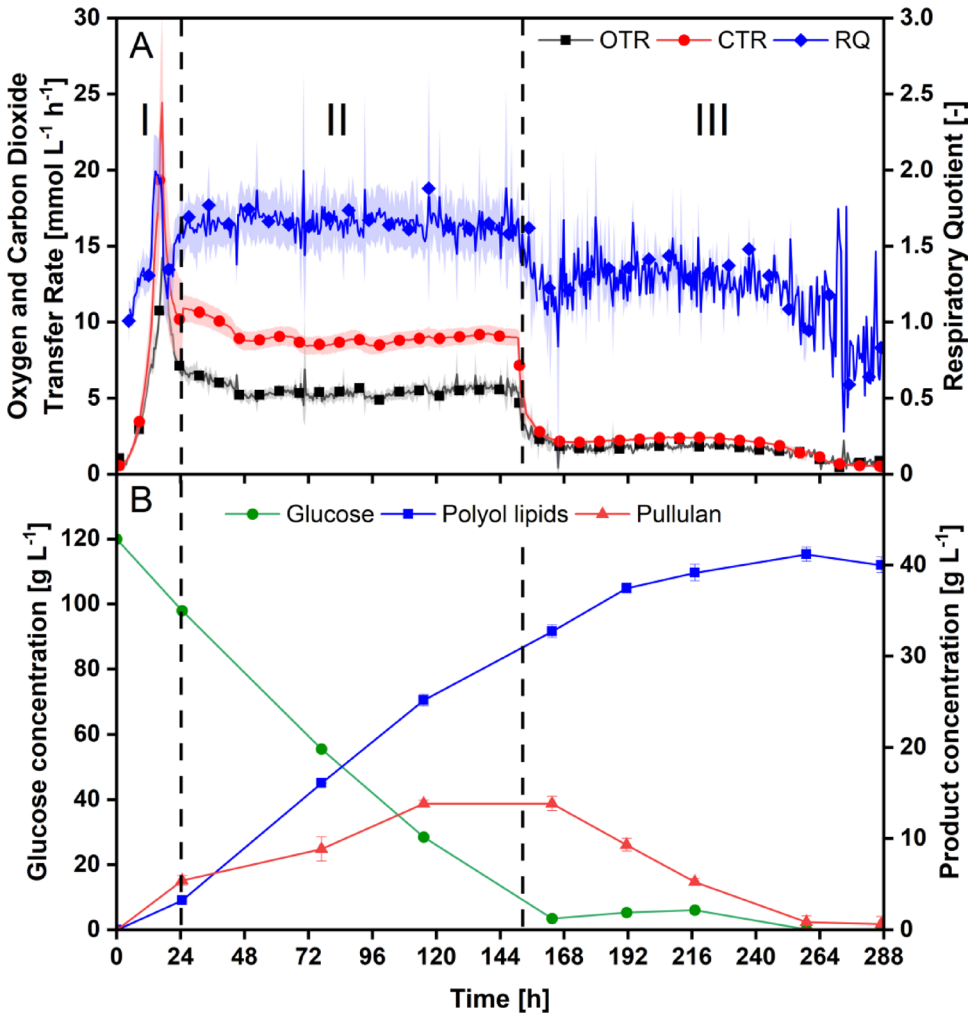

Fig. 1 Different metabolic phases during PL production. (**A**) OTR, CTR, RQ, (**B**) glucose, pullulan, and PL concentrations during a shake flask cultivation of *Aureobasidium pullulans* NRRL 62042. Cultivation conditions were: MLP medium, 120 g L^{-1} glucose, 20 mL filling volume, 30 °C, 350 rpm, Kuhner TOM. For clarity, symbols were only drawn every 15th datapoint for (A). Standard deviation is indicated by shadows (A) or error bars (B). Cultivation can be divided into three phases: (I) growth (II) PL and pullulan production on glucose (III) PL production on residual pullulan. PL: polyol lipid, OTR: oxygen transfer rate, CTR: carbon dioxide transfer rate, RQ: respiratory quotient

declining to a plateau at 5 and 8 mmol L^{-1} h^{-1}, respectively. This OTR course was described as typical for cultures with a secondary substrate limitation [38]. In this case, a nitrogen limitation was introduced by the high carbon-to-nitrogen ratio in the medium, ultimately stopping cell growth, which results in a decline in respiratory activity [23]. During the growth phase, 20 g L^{-1} glucose were consumed, and 3.2 g L^{-1} PLs and 5.4 g L^{-1} pullulan were formed (see Fig. 1B).

In phase II, the respiratory activity remained constant with an OTR and CTR of 5.3 and 9 mmol L^{-1} h^{-1}, resulting in an RQ value of 1.7. PL and pullulan concentrations increased with a linear kinetic in this phase to values of 32.7 and 13.8 g L^{-1}, respectively. Since respiratory activity did not decrease with the linear production of PL biosurfactants, the gas transfer was not negatively affected by PL production. PLs possess a high degree of reduction per carbon atom, with 5–5.2 (depending on the congener) [23]. Thus, an RQ above 1 is expected for the formation of PL congeners, using glucose as carbon source. Moreover, *A. pullulans* can produce intracellular storage lipids after growth, which also contributes to the observed RQ values above 1 because of their reduced nature. Changes in CDW during phase II after growth had ceased (see Supplementary Information Fig. S2) could be attributed to intracellular lipid formation and were comparable to values reported by Haala et al. [23]. The RQ recorded during the production of microbial triglycerides, which are other reduced intracellular lipids, in *Ustilago maydis*, was also reported to be above 1.0 by Richter et al. [45], further supporting this claim. After 152 h, a sharp drop in respiratory activity marks the end of this phase, indicating depletion of the main carbon source glucose [38]. Glucose concentrations at the end of phase II did not reach 0 g L^{-1} in the samples analyzed in this experiment, but respiration activity indicated its depletion, and the sample taken after 163 h was likely already influenced by the onset of glucose release due to pullulan degradation. *A. pullulans* degrading pullulan while simultaneously releasing glucose again was already reported in literature [46]. As illustrated in Fig. S1, glucose is released during pullulan degradation catalyzed by a glucoamylase, and the released glucose can be taken up again and subsequently be used for further PL production.

In the following phase III, OTR and CTR dropped to values between 2 and 3 mmol L^{-1} h^{-1}, until ultimately declining to nearly zero after 264 h. RQ values were around 1.3 during this phase, which is lower compared to phase II. The RQ was still above 1.0, indicating further production of reduced components. This was confirmed by the increasing PL titer in this phase, as discussed before. Compared to phase II, the PL formation took place at a slower rate, which explains the lower respiratory activity in this phase. Furthermore, CDW recorded during this phase (see Supplementary Information Fig. S2) did not increase further, indicating that little to no additional intracellular lipids were formed during this phase. Overall, this likely resulted in a lower RQ compared to phase II, where PLs and intracellular lipids were produced at the same time. Glucose levels stabilized around 5 g L^{-1} while the remaining pullulan was consumed again by the organism, producing more PLs. After 264 h, all remaining pullulan and glucose were finally depleted, and a final PL titer of 40 g L^{-1} with a yield ($Y_{P/S}$) of 0.33 g PLs per g of glucose and a space time yield of 0.14 g L^{-1} h^{-1} was reached. The PL production process performed in this work is in accordance with literature. PL production mainly took place after cell growth (e.g., under nitrogen-limited conditions in phases II and III) as previously described by Manitchotpisit et al. [24]. Haala et al. [23] observed a similar course of respiration activity during fermentations of the same *A. pullulans* strain with a nitrogen-limited medium of almost the same composition. They also observed glucose depletion coinciding with a drop in the OTR. Although they did not cultivate until pullulan was fully consumed, they also observed its beginning degradation after the initial glucose was depleted. The three-phase PL production process characterized in this chapter will now be further evaluated regarding the possibility of fluorescence-based online monitoring of PL formation.

3.2 Unraveling the fluorescent properties of the PL phase

The oily PL phase secreted by *A. pullulans* has been described as highly fluorescent in literature and the yellow color of the broth gave this genus its name. Manitchotpisit et al. [24] observed a bright yellow, fluorescing PL phase under a fluorescence microscope. In this work, the fluorescent properties of the PL phase produced by the wild-type strain *A. pullulans* NRRL 62042 in the reference process (Fig. 1) were evaluated for their online monitoring suitability. From the PLs produced during the reference process, solutions were prepared of the dried PL phase in a mix of acetonitrile and deionized water (60:40 vol%). 2D fluorescence spectra of these solutions were recorded using an in-house-built 2D-BioLector [36, 37]. The resulting difference spectrum (Fig. 2) showed three main areas of fluorescence.

The strongest fluorescence was observed for area 1 with intensities of up to 1,500 a.u. at excitation wavelengths ranging from λ_{ex} = 320 to 360 nm and emission wavelengths of λ_{em} = 430 to 565 nm. The second prominent fluorescence area (area 2) was observed at λ_{ex} = 470 to 540 nm and λ_{em} = 540 to 580 nm with intensities between 750 and 1,000 a.u. A third notable, but less prominent, fluorescent spot (area 3) could be observed around λ_{ex} = 400 nm and λ_{em} = 630 nm. The structure of PL congeners does not contain any

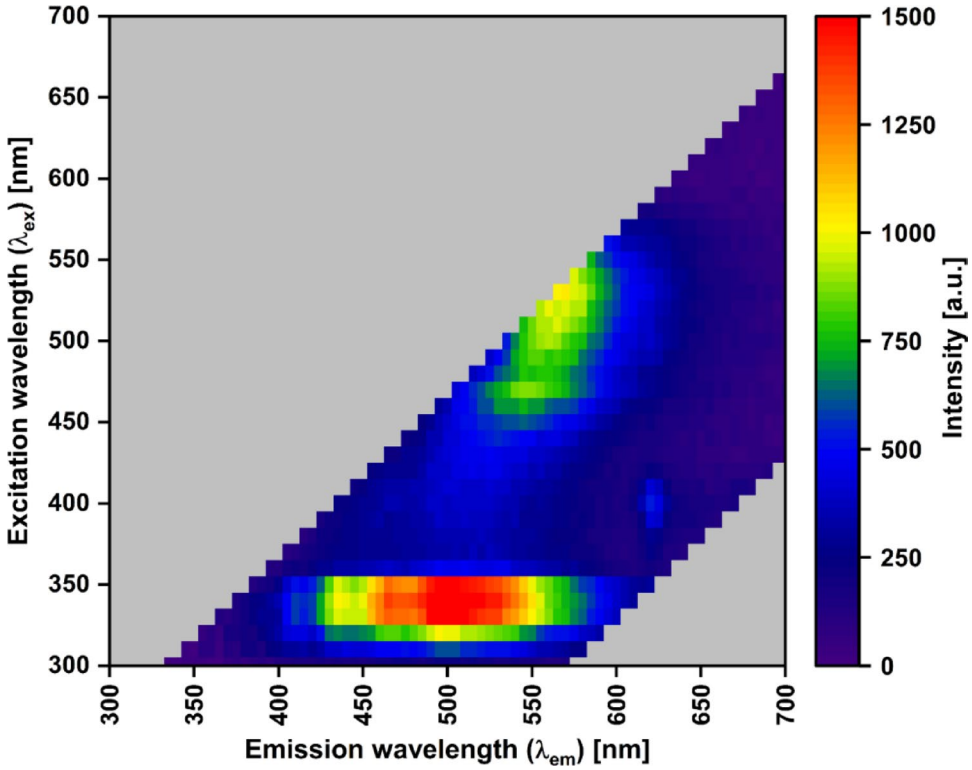

Fig. 2 Mean 2D fluorescence difference spectrum of polyol lipid (PL) solutions produced during shake flask cultivation. 2D-BioLector measurements (mean of $n = 12$) at 1,000 rpm at 30 °C. Spectroscopic measurement settings: excitation wavelength range = 270–700 nm, excitation step size = 10 nm, emission wavelength range = 270–700 nm, emission step size = 5 nm, integration time = 600 ms. The area 30 nm around the scattered light ($\lambda_{ex} = \lambda_{em}$) was cut off. Data was referenced to the mean spectrum of the solvent without PLs. Unmeasured areas are shown in gray

fluorescence-associated structures like conjugated double bonds or aromatic rings [21]. Thus, there is no evidence for PLs having fluorescent properties themselves, suggesting the observed fluorescence likely results from other fluorescent molecules also produced by *A. pullulans.* Due to the extraction method used for the purification of PLs in this work, it is highly possible that cell-associated fluorescent components like cofactors, vitamins, or pigments were also extracted from the cell pellet. The observed fluorescence could also be a result of these components being incorporated into the oily PL phase.

Fluorescence in area 1 matches fluorescence likely originating from intracellular compounds like cofactors or vitamins, e.g., NADH or pyridoxine, which can be measured using wavelength combinations ($\lambda_{ex}/\lambda_{em}$) of 340/460 nm and 330/390 nm, respectively [31, 47, 48]. Furthermore, Manitchotpisit et al. [24] observed fluorescence for the PL phase produced by *A. pullulans* strain CU 43 when excited at 365 nm, which is close to the excitation range of area 1.

The second fluorescing area (area 2) could be the result of flavins, which are known to show fluorescent behavior in a range near area 2 [34, 47]. Other potential sources of fluorescence could be fungal pigments [35] or siderophores [18, 49] and precursors thereof, which are produced by many fungi. *Aureobasidium* is a known producer of 1,8-dihydroxynaphthalene melanin and various precursors like 1,3,6,8-tetrahydroxynaphthalene, 1,3,8-trihydroxynaphthalene, and scytalone [50]. Conjugated double bonds and aromatic rings in those precursor molecules could also result in fluorescent properties. However, analyses of PL phases produced by various *A. pullulans* strains done by Manitchotpisit et al. [24] indicated that the fluorescing compound is not riboflavin and there were no aromatic groups present. It could be possible that *A. pullulans* produces fluorescent pigments similar to undecylprodigiosin and actinorhodin produced by the fungal model organism *Streptomyces coelicolor* A3 (2). For this organism, Finger et al. [35] reported autofluorescence at 483/520 nm ($\lambda_{ex}/\lambda_{em}$), which is near the fluorescence observed for area 2. Other pigments could result in similar or slightly shifted fluorescence patterns.

Fluorescence in area 3 could likely be the result of porphyrins. Porphyrins, such as protoporphyrin IX and hematoporphyrin, exhibit fluorescence matching that of area 3 with an excitation wavelength of 400 nm and emission at around 600–630 nm [48, 51–53]. For *A. pullulans*, the presence of genes encoding porphyrin biosynthesis was reported by Gostinčar et al. [11].

Although the origin of the fluorescence could not be precisely identified, it appears to be co-expressed with the product of interest. For this reason, time-resolved monitoring of fluorescence area 2 in the reference process presented in Sect. 3.1 will be carried out in the following chapter. To validate whether the increased fluorescence is a result of PL formation, a PL-negative strain will be cultivated alongside the wild-type strain.

3.3 Correlation of fluorescence signals and PL production

Multiple wavelength combinations in the identified areas were tested for their suitability for time-resolved online monitoring of the PL production in MTP cultivations. To evaluate possible correlations between fluorescence and PL titer, *A. pullulans* was cultivated in the µRAMOS-BioLector combination, an in-house-built device capable of monitoring OTR and fluorescence in each well of a 48-well MTP [42]. During cultivation, samples were drawn from offline MTPs, which were cultivated under the same conditions, but without online monitoring. Time-resolved data from this experiment are shown in Fig. 3. For fluorescence, of all tested wavelengths, only data for the wavelength combination with the best correlation between fluorescence intensity and PL titer (λ_{ex} = 540 nm, λ_{em} = 580 nm), which could also be successfully validated later, are shown. An overview of correlations obtained from the measurement at other tested wavelengths is provided in Supplementary Information Fig. S3 and Table S1.

The OTR course and PL titers observed in the MTP cultivation (Fig. 3) are comparable to those observed during shake flask cultivation (Fig. 1), indicating a successful scale-down of the shake flask process into milliliter scale. The three phases of the PL production process were also clearly observable. PL formation (Fig. 3B) during the first production phase (phase II) was linear, reaching concentrations of 33 g L^{-1} after 141 h. In phase III, the increase in PLs was slower compared to phase II, ultimately reaching 41 g PLs L^{-1}. Overall, there were two different kinetics of PL formation visible in phases II and III. The blanked fluorescence signal (Fig. 3B) exhibited a similar trend to the observed PL titer in the MTP cultivation. Non-blanked fluorescence data of this experiment are shown in Supplementary Information Fig. S4B. In phase II, fluorescence increased with a linear kinetic to values of 4 a.u., followed by a slower increase during phase III, reaching a saturation at 6 a.u. As all fluorescence signals used in this work are relative values expressed as arbitrary units and were measured with different spectroscopic setups, the absolute values of the 2D fluorescence (Fig. 2) and the online fluorescence (Fig. 3) are not comparable.

As has been discussed previously, offline data for this cultivation (Supplementary Information Fig. S4) confirmed that PLs and pullulan were formed until glucose was depleted, followed by a second production phase utilizing the remaining pullulan. These two phases were also clearly distinguishable in the recorded fluorescence at λ_{ex} = 540 nm and λ_{em} = 580 nm. To evaluate the possible correlation, the

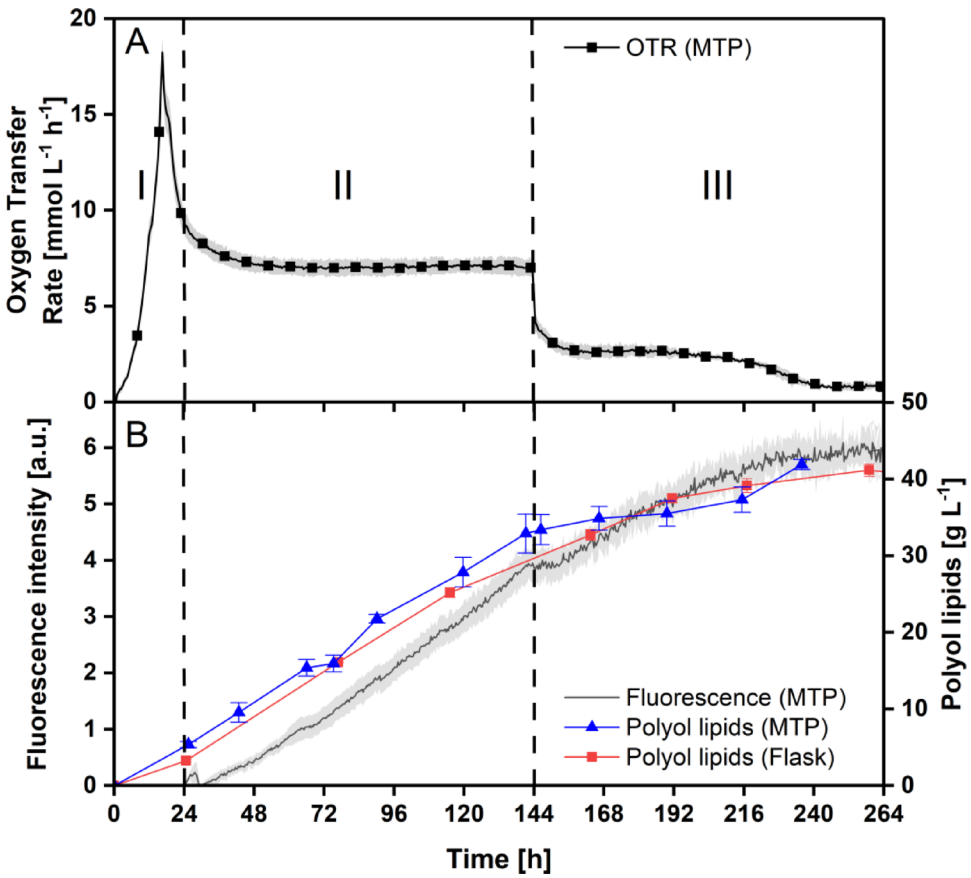

Fig. 3 Time-resolved fluorescence-based monitoring of polyol lipid (PL) formation during MTP cultivation. (**A**) Oxygen transfer rate, (**B**) fluorescence intensity (λ_{ex} = 540 nm, λ_{em} = 580 nm), and PL concentrations during PL production. Data shown were obtained during MTP cultivations in the µRAMOS-BioLector combination. OTR and fluorescence are presented as means of six biological replicates. PL concentrations during shake flask cultivation (red) were added for comparison. Cultivation conditions: *Aureobasidium pullulans* NRRL 62042, MLP medium, 120 g L^{-1} glucose, 30 °C, 1,000 rpm, 1 mL per well, 48-well MTP. Standard deviations are indicated by shadows or error bars. For clarity, symbols were only drawn every 15th datapoint for (A). Fluorescence intensities were referenced to values measured at 24 h of cultivation. Cultivation can be divided into three phases: (I) growth, (II) PL and pullulan production on glucose, and (III) PL production on residual pullulan. MTP: microtiter plate, OTR: oxygen transfer rate

recorded fluorescence data were plotted over the respective PL titer (Fig. 4). A linear fit was applied to this plot, confirming a strong correlation between PL titer and fluorescence during phases II and III, with an R^2 value of 0.96, representing a linear correlation.

To validate that the observed change in fluorescence is a result of PL formation, a PL-negative strain (*A. pullulans* VA.Y1, Dielentheis-Frenken et al., unpublished data) was cultivated in the µRAMOS-BioLector device. Time-resolved online data for this cultivation are shown in Fig. 5. For both strains, OTR during growth in phase I behaved similarly to the reference MTP experiment (Fig. 3A). In phase II, both strains stopped growing due to a nitrogen limitation, visible in the OTR as previously discussed. Plateaus in this phase differed in height, with OTRs of 8 and 6 mmol L^{-1} h^{-1} for wildtype and mutant strain, respectively. In phase III, the OTR marked glucose depletion for the wild-type strain with subsequent pullulan consumption similar to the previous reference experiment (Fig. 3). However, with the glucose-related drop in OTR taking place after 120 h, phase II ended earlier than in the reference experiment because the initial glucose concentration was lowered to 100 g L^{-1} in this cultivation. In contrast to the wildtype, the OTR plateau observed for the PL-negative strain was prolonged and did not drop until the end of the cultivation after 300 h, suggesting a lower carbon uptake rate. This is supported by HPLC measurements, which revealed that glucose was fully consumed in wild-type cultures, while 18 g L^{-1} glucose remained in cultures of the knockout strain after 300 h. The overall lower respiration activity of the mutant strain during phase II is likely because no PLs can be produced by the strain. Thus, glucose consumption and therefore metabolic activity are lowered, ultimately resulting in a lower OTR compared to the wild-type strain.

Fluorescence recorded for the wild-type cultures (Fig. 5B, black line) showed the expected course during phases II and III, ultimately reaching 6.5 a.u. Contrastingly, the fluorescence recorded for the non-producing strain (Fig. 5B, red line) was much lower, with up to 1 a.u., and showed a lower increase over time. At the end of the cultivation, the wild-type strain had produced 31 g L^{-1} of PLs, while for the knockout strain, no PLs were detectable. Since the PL phase accumulates at the bottom of the MTP wells because of its high density, PL formation (or the absence of such) could be easily confirmed visually at the end of cultivation (Supplementary Information Fig. S5). This phenomenon is likely also a reason for the change in fluorescence intensity during production.

Fluorescence measurements at λ_{ex} = 540 nm and λ_{em} = 580 nm could successfully be validated for qualitative online monitoring of PL formation in *A. pullulans* without sampling. Fluorescence signals were confirmed to correlate with and be the result of PL formation after growth ceased, with the chosen wavelength combination only displaying negligible changes during cultivations where no PLs were produced. In general, PL titer and fluorescence showed a strong linear correlation, which could be used in future experiments to monitor PL production during cultivation, eliminating the need for laborious sampling. During future strain optimization, a careful

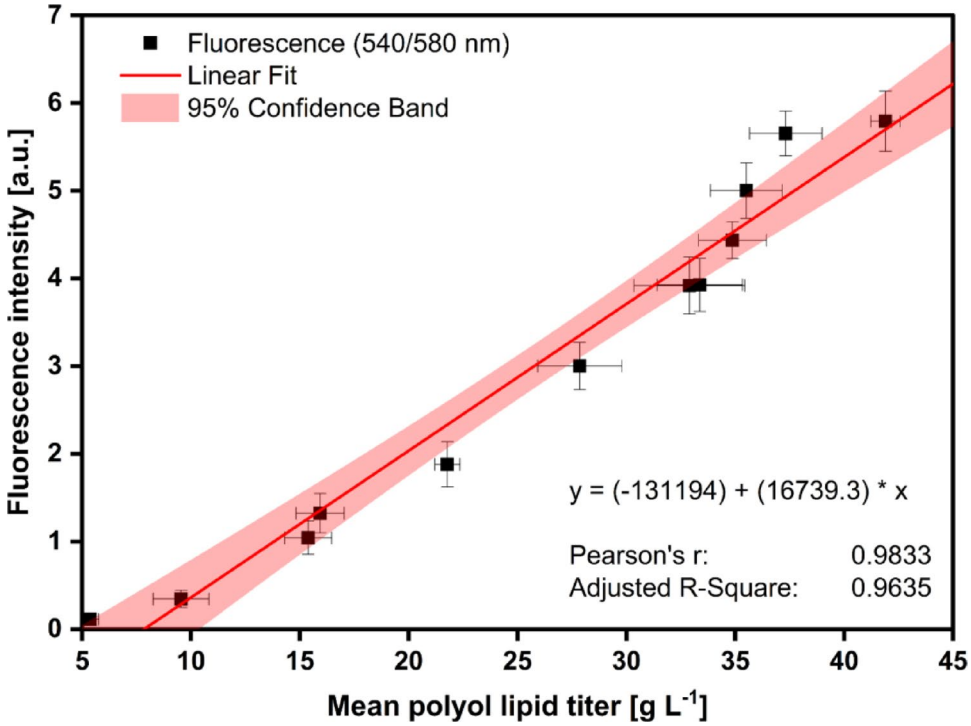

Fig. 4 Mean fluorescence intensity over PL titer in MTP cultivation. Data were fitted using OriginPro 2022 (OriginLab). Fluorescence (λ_{ex} = 540 nm, λ_{em} = 580 nm) was normalized to whole numbers for more clarity. Error bars indicate the standard deviation (Fluorescence: n = 6, PL titer: n = 3). Cultivation conditions: *Aureobasidium pullulans* NRRL 62042, MLP medium, 120 g L^{-1} glucose, 30 °C, 1,000 rpm, 1 mL per well, 48-well MTP. PL: polyol lipid, MTP: microtiter plate

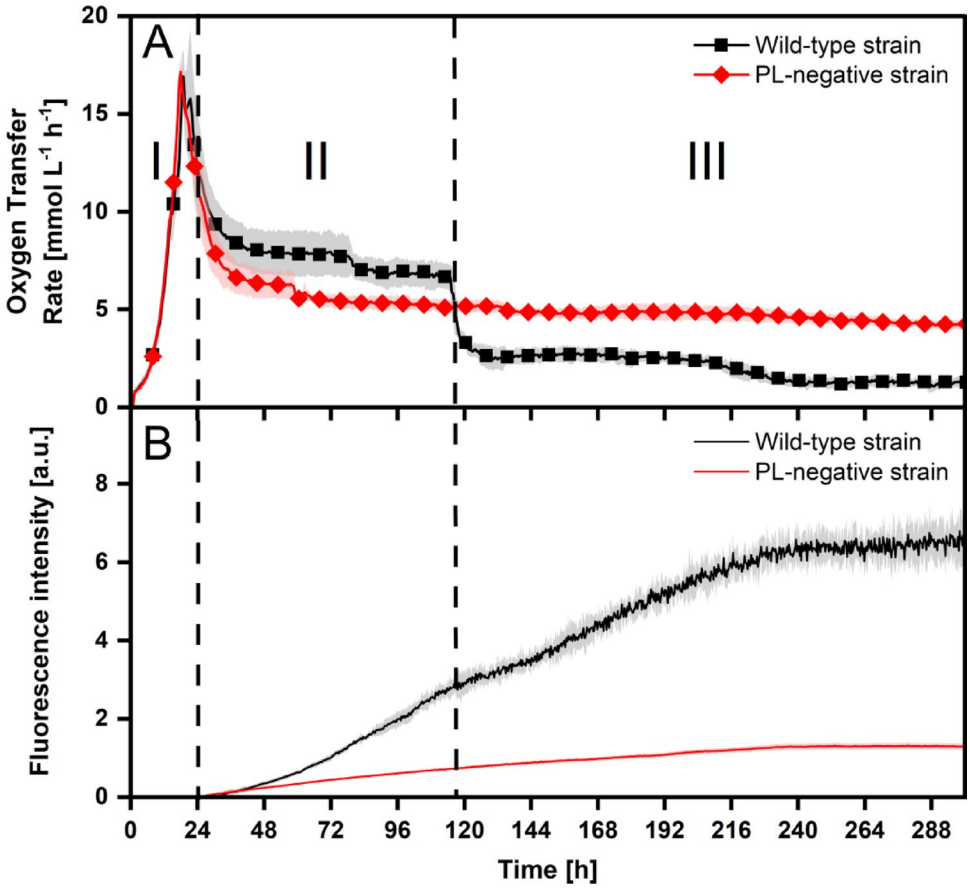

Fig. 5 Time-resolved data of a validation experiment with a PL-negative strain and the wild-type organism. Cultivation in µRAMOS-BioLector combination: *Aureobasidium pullulans* NRRL 62042 (Wildtype) or *A. pullulans* VA.Y1 (PL-negative), 30 °C, 3 mm, 1,000 rpm, 1 mL per well, MLP medium, 100 g L^{-1} glucose. Fluorescence values were measured at λ_{ex} = 540 nm, λ_{em} = 580 nm, and were referenced to values measured at 24 h of cultivation. OTR and fluorescence are presented as mean values of six biological replicates. Shadows indicate standard deviation. Cultivation can be divided into three phases: (I) growth, (II) PL and pullulan production on glucose, and (III) PL production on residual pullulan. PL: polyol lipid, OTR: oxygen transfer rate

reevaluation of the correlation between fluorescent properties of the modified strains and their PL production will be necessary since genetic modifications could potentially alter the fluorescence profile of the strain. To ensure the validity of the monitoring method, an iterative reevaluation of the correlation between fluorescence and PL titer after each genetic modification will be possible with the methodology presented in our work.

4 Conclusion

In this study, the PL production with *A. pullulans* was analyzed with regard to potential fluorescent properties. This resulted in the first ever-reported method for online monitoring of PL production in small-scale cultivations of *A. pullulans*. Based on respiratory activity, the PL production process in *A. pullulans* NRRL 62042 was characterized, and three distinct phases were identified: growth, simultaneous production of PLs and pullulan on glucose, and production on residual pullulan. 2D fluorescence of PLs produced in shake flask cultivation was analyzed, and possible wavelength combinations for online monitoring were identified and tested. It was shown that PL titer correlates strongly with fluorescence measured at λ_{ex} = 540 nm and λ_{em} = 580 nm. Using online fluorescence measurement, two distinct kinetics of PL production could be observed in phases II and III of the process. The chosen wavelength combination was validated by cultivating a PL-negative mutant strain of *A. pullulans*, which showed no significant increase in fluorescence over time. With this novel method, fluorescence presents a continuous signal for PL formation, and sampling efforts during cultivations can be significantly reduced, as laborious extraction of the PLs from the culture broth is not necessary. Additionally, the use of MTPs for cultivation provides higher experimental throughput compared to standard lab-scale reactors or even shake flask cultivations. The here presented PL online monitoring enables studies with increased experimental throughput, such as isolate characterization and mutant performance screening, all contributing to an accelerated development of a sustainable PL biosurfactant production process.

Supplementary Information The online version contains supplementary material available at https://doi.org/10.1007/s12257-026-00264-8.

Acknowledgements The authors are grateful to René Petri (Aachener Verfahrenstechnik – Chair of Biochemical Engineering) for supporting with HPLC measurements. This work was funded by the Ministry of Culture and Science of the German State of North Rhine-Westphalia

within the framework of the NRW Strategieprojekt BioSC (Grant/Award Number: 313/323-400-002 13). Open Access funding enabled and organized by Projekt DEAL.

Author contributions Conceptualizing [MDD], Methodology [MDD], Formal analysis and investigation [MDD, NLJC], writing – original draft preparation [MDD], Writing – review and editing [MDD, NLJC, PK, MD-F, LMB, VS, MM, TT, JBM], Resources [LMB, MM, TT, JBM], Supervision [VS, MM, JBM].

Funding Open Access funding enabled and organized by Projekt DEAL.

Declarations

competing interests The authors declare the following competing financial interests: MD-F, LMB and TT declare that a patent application related to thesubject matter of this manuscript has been filed. Additionally, TT is a co-founder and CTO of a company which aims to commercializebiomanufacturing processes related to the work presented in this study.

Open Access This article is licensed under a Creative Commons Attribution 4.0 International License, which permits use, sharing, adaptation, distribution and reproduction in any medium or format, as long as you give appropriate credit to the original author(s) and the source, provide a link to the Creative Commons licence, and indicate if changes were made. The images or other third party material in this article are included in the article's Creative Commons licence, unless indicated otherwise in a credit line to the material. If material is not included in the article's Creative Commons licence and your intended use is not permitted by statutory regulation or exceeds the permitted use, you will need to obtain permission directly from the copyright holder. To view a copy of this licence, visit http://creativecommons.org/licenses/by/4.0/.

References

1. Cowan-Ellsberry C, Belanger S, Dorn P et al (2014) Environmental safety of the use of major surfactant classes in North America. Crit Rev Environ Sci Technol 44:1893–1993. https://doi.org/10.1080/10739149.2013.803777
2. Banat IM, Franzetti A, Gandolfi I et al (2010) Microbial biosurfactants production, applications and future potential. Appl Microbiol Biotechnol 87:427–444. https://doi.org/10.1007/s00253-010-2589-0
3. Cameotra SS, Makkar RS (2004) Recent applications of biosurfactants as biological and immunological molecules. Curr Opin Microbiol 7:262–266. https://doi.org/10.1016/j.mib.2004.04.006
4. Henkel M, Hausmann R (2019) Diversity and classification of microbial surfactants. In: Hayes DG, Solaiman DKY, Ashby RD (eds) Biobased surfactants. Academic Press and AOCS Press, London, pp 41-63https://doi.org/10.1016/B978-0-12-812705-6.00002-2
5. Paulino BN, Pessôa MG, Mano MC et al (2016) Current status in biotechnological production and applications of glycolipid biosurfactants. Appl Microbiol Biotechnol 100:10265–10293. https://doi.org/10.1007/s00253-016-7980-z
6. Invally K, Ju L (2020) Increased rhamnolipid concentration and productivity achieved with advanced process design. J Surfactants Deterg 23:1043–1053. https://doi.org/10.1002/jsde.12457
7. Evonik Industries AG (2024) Evonik manufactures first product from world's first industrial-scale rhamnolipid biosurfactant plant - Evonik Industries. https://personal-care.evonik.com/en/evonik-manufactures-first-product-from-worlds-first-industrial-scale-rhamnolipid-biosurfactant-plant-233324.html. Accessed 25 March 2025
8. Kurosawa T, Sakai K, Nakahara T et al (1994) Extracellular accumulation of the polyol lipids, 3,5-dihydroxydecanoyl and 5-hydroxy-2-decenoyl esters of arabitol and mannitol, by *Aureobasidium* sp. Biosci Biotechnol Biochem 58:2057–2060. https://doi.org/10.1271/bbb.58.2057
9. Schoch CL, Shoemaker RA, Seifert KA et al (2006) A multigene phylogeny of the dothideomycetes using four nuclear loci. Mycologi 98:1041–1052. https://doi.org/10.3852/mycologia.98.6.1041
10. Prasongsuk S, Lotrakul P, Ali I et al (2018) The current status of *Aureobasidium pullulans* in biotechnology. Folia Microbiol (Praha) 63:129–140. https://doi.org/10.1007/s12223-017-0561-4
11. Gostinčar C, Turk M, Zajc J et al (2019) Fifty *Aureobasidium pullulans* genomes reveal a recombining polyextremotolerant generalist. Environ Microbiol 21:3638–3652. https://doi.org/10.1111/1462-2920.14693
12. Xiao D, Driller M, Dielentheis-Frenken M et al (2024) Advances in *Aureobasidium* research: paving the path to industrial utilization. Microb Biotechnol 17:e14535. https://doi.org/10.1111/1751-7915.14535
13. Leathers TD (1989) Purification and properties of xylanase from *Aureobasidium*. J Ind Microbiol 4:341–348. https://doi.org/10.1007/BF01569536
14. Leathers TD, Price NP, Manitchotpisit P et al (2016) Production of anti-streptococcal liamocins from agricultural biomass by *Aureobasidium pullulans*. World J Microbiol Biotechnol 32:199. https://doi.org/10.1007/s11274-016-2158-5
15. Leathers TD (2003) Biotechnological production and applications of pullulan. Appl Microbiol Biotechnol 62:468–473. https://doi.org/10.1007/s00253-003-1386-4
16. Li B, He J, Zuo K et al (2024) Engineering the by-products pathway in *Aureobasidium pullulans* for highly purified polymalic acid fermentation with concurrent recovery of l-malic acid. Bioresour Technol 414:131578. https://doi.org/10.1016/j.biortech.2024.131578
17. Gessler NN, Egorova AS, Belozerskaya TA (2014) Melanin pigments of fungi under extreme environmental conditions (review). Appl Biochem Microbiol 50:105–113. https://doi.org/10.7868/s0555109914020093
18. Wang WL, Chi ZM, Chi Z et al (2009) Siderophore production by the marine-derived *Aureobasidium pullulans* and its antimicrobial activity. Bioresour Technol 100:2639–2641. https://doi.org/10.1016/j.biortech.2008.12.010
19. Campana R, Fanelli F, Sisti M (2022) Role of melanin in the black yeast fungi *Aureobasidium pullulans* and *Zalaria obscura* in promoting tolerance to environmental stresses and to antimicrobial compounds. Fungal Biol 126:817–825. https://doi.org/10.1016/j.funbio.2022.11.002
20. Tiso T, Welsing G, Lipphardt A et al (2024) Proposal for a systematic naming convention for liamocins. J Surfactants Deterg 27:459–461. https://doi.org/10.1002/jsde.12735
21. Price NPJ, Manitchotpisit P, Vermillion KE et al (2013) Structural characterization of novel extracellular liamocins (mannitol oils) produced by *Aureobasidium pullulans* strain NRRL 50380. Carbohydr Res 370:24–32. https://doi.org/10.1016/j.carres.2013.01.014
22. Price NP, Bischoff KM, Leathers TD et al (2017) Polyols, not sugars, determine the structural diversity of anti-streptococcal liamocins produced by *Aureobasidium pullulans* strain NRRL 50380. J Antibiot 70:136–141. https://doi.org/10.1038/ja.2016.92
23. Haala F, Dielentheis-Frenken MRE, Brandt FM et al (2024) DoE-based medium optimization for improved biosurfactant

production with *Aureobasidium pullulans*. Front Bioeng Biotechnol 12:1379707. https://doi.org/10.3389/fbioe.2024.1379707
24. Manitchotpisit P, Price NP, Leathers TD et al (2011) Heavy oils produced by *Aureobasidium pullulans*. Biotechnol Lett 33:1151–1157. https://doi.org/10.1007/s10529-011-0548-1
25. Kim JS, Lee IK, BS (2015) A novel biosurfactant produced by *Aureobasidium pullulans* L3-GPY from a tiger Lily wild flower, lilium lancifolium thunb. PLoS ONE 10:e0122917. https://doi.org/10.1371/journal.pone.0122917
26. Nitschke M, Costa SGVAO, Contiero J (2005) Rhamnolipid surfactants: an update on the general aspects of these remarkable biomolecules. Biotechnol Prog 21:1593–1600. https://doi.org/10.1021/bp050239p
27. Bischoff KM, Leathers TD, Price NP et al (2015) Liamocin oil from *Aureobasidium pullulans* has antibacterial activity with specificity for species of Streptococcus. J Antibiot 68:642–645. https://doi.org/10.1038/ja.2015.39
28. Manitchotpisit P, Watanapokasin R, Price NPJ et al (2014) *Aureobasidium pullulans* as a source of Liamocins (heavy oils) with anticancer activity. World J Microbiol Biotechnol 30:2199–2204. https://doi.org/10.1007/s11274-014-1639-7
29. Bhatta H, Goldys EM, Learmonth RP (2006) Use of fluorescence spectroscopy to differentiate yeast and bacterial cells. Appl Microbiol Biotechnol 71:121–126. https://doi.org/10.1007/s00253-005-0309-y
30. Palacio-Barrera AM, Schlembach I, Finger M et al (2022) Reliable online measurement of population dynamics for filamentous co-cultures. Microb Biotechnol 15:2773–2785. https://doi.org/10.1111/1751-7915.14129
31. Samorski M, Müller-Newen G, Büchs J (2005) Quasi-continuous combined scattered light and fluorescence measurements: a novel measurement technique for shaken microtiter plates. Biotechnol Bioeng 92:61–68. https://doi.org/10.1002/bit.20573
32. Kunze M, Roth S, Gartz E et al (2014) Pitfalls in optical on-line monitoring for high-throughput screening of microbial systems. Microb Cell Fact 13:53. https://doi.org/10.1186/1475-2859-13-53
33. Kensy F, Zang E, Faulhammer C et al (2009) Validation of a high-throughput fermentation system based on online monitoring of biomass and fluorescence in continuously shaken microtiter plates. Microb Cell Fact 8:31. https://doi.org/10.1186/1475-2859-8-31
34. Wandrey G, Wurzel J, Hoffmann K et al (2016) Probing unnatural amino acid integration into enhanced green fluorescent protein by genetic code expansion with a high-throughput screening platform. J Biol Eng 10:11. https://doi.org/10.1186/s13036-016-0031-6
35. Finger M, Sentek F, Hartmann L et al (2023) Insights into *Streptomyces coelicolor* A3(2) growth and pigment formation with high-throughput online monitoring. Eng Life Sci 23:e2100151. https://doi.org/10.1002/elsc.202100151
36. Berg C, Busch S, Alawiyah MD et al (2023) Advancing 2D fluorescence online monitoring in microtiter plates by separating scattered light and fluorescence measurement, using a tunable emission monochromator. Biotechnol Bioeng 120:2925–2939. https://doi.org/10.1002/bit.28474
37. Berg C, Ihling N, Finger M et al (2022) Online 2D fluorescence monitoring in microtiter plates allows prediction of cultivation parameters and considerable reduction in sampling efforts for parallel cultivations of *Hansenula polymorpha*. Bioengineering 9:438. https://doi.org/10.3390/bioengineering9090438
38. Anderlei T, Büchs J (2001) Device for sterile online measurement of the oxygen transfer rate in shaking flasks. Biochem Eng J 7:157–162. https://doi.org/10.1016/s1369-703x(00)00116-9
39. Anderlei T, Zang W, Papaspyrou M et al (2004) Online respiration activity measurement (OTR, CTR, RQ) in shake flasks. Biochem Eng J 17:187–194. https://doi.org/10.1016/s1369-703x(03)00181-5
40. Schulte A, Brockmann J, Müller N et al (2025) A new approach to off-gas analysis for shaken bioreactors showing high CTR and RQ accuracy. J Biol Eng 19:11. https://doi.org/10.1186/s13036-025-00480-5
41. Heyman B, Tulke H, Putri SP et al (2020) Online monitoring of the respiratory quotient reveals metabolic phases during microaerobic 2,3-butanediol production with *Bacillus licheniformis*. Eng Life Sci 20:133–144. https://doi.org/10.1002/elsc.201900121
42. Ladner T, Held M, Flitsch D et al (2016) Quasi-continuous parallel online scattered light, fluorescence and dissolved oxygen tension measurement combined with monitoring of the oxygen transfer rate in each well of a shaken microtiter plate. Microb Cell Fact 15:206. https://doi.org/10.1186/s12934-016-0608-2
43. Sparviero S, Dicke MD, Rosch TM et al (2023) Yeast extracts from different manufacturers and supplementation of amino acids and micro elements reveal a remarkable impact on alginate production by *A. vinelandii* ATCC9046. Microb Cell Fact 22:99. https://doi.org/10.1186/s12934-023-02112-3
44. Steimann T, Wollborn D, Röck F et al (2024) Investigation into struvite precipitation: a commonly encountered problem during fermentations on chemically defined media. Biotechnol Bioeng 121:1076–1089. https://doi.org/10.1002/bit.28633
45. Richter P, Maßjosthusmann M, Seidel T et al (2025) Tailoring the fatty acid profile of microbial triglycerides in *Ustilago maydis* by adapting the cultivation conditions. Bioresource Technol Rep 30:102119. https://doi.org/10.1016/j.biteb.2025.102119
46. West TP, Strohfus B (1996) A pullulan-degrading enzyme activity of *Aureobasidium pullulans*. J Basic Microbiol 36:377–380. https://doi.org/10.1002/jobm.3620360513
47. Masiero SS, Trierweiler JO, Farenzena M et al (2013) Evaluation of wavelength selection methods for 2D fluorescence spectra applied to bioprocesses characterization. Braz J Chem Eng 30:289–298. https://doi.org/10.1590/s0104-66322013000200007
48. Christensen J, Nørgaard L, Bro R et al (2006) Multivariate autofluorescence of intact food systems. Chem Rev 106:1979–1994. https://doi.org/10.1021/cr050019q
49. Renshaw JC, Robson GD, Trinci APJ et al (2002) Fungal siderophores: structures, functions and applications. Mycol Res 106:1123–1142. https://doi.org/10.1017/s0953756202006548
50. Gostinčar C, Ohm RA, Kogej T et al (2014) Genome sequencing of four *Aureobasidium pullulans* varieties: biotechnological potential, stress tolerance, and description of new species. BMC Genomics 15:549. https://doi.org/10.1186/1471-2164-15-549
51. Wlodarski M, Kaliszewski M, Kwasny M et al (2006) Fluorescence excitation-emission matrices of selected biological materials. In: Carrano JC, Zukauskas A (eds) Optically based biological and chemical detection for defence III. SPIE, Bellingham, pp 11-22 https://doi.org/10.1117/12.687872
52. DaCosta RS, Andersson H, Wilson BC (2003) Molecular fluorescence excitation-emission matrices relevant to tissue spectroscopy. Photochem Photobiol 78:384–392. https://doi.org/10.1562/0031-8655(2003)0780384MFEMRT2.0.CO2
53. Lennon ÁM, Brune L, Techert S et al (2023) Fluorescence spectroscopy shows porphyrins produced by cultured oral bacteria differ depending on composition of growth media. Caries Res 57:74–86. https://doi.org/10.1159/000528731

Publisher's Note Springer Nature remains neutral with regard to jurisdictional claims in published maps and institutional affiliations.